BRL

NUMERICAL SIMULATION AND MODELING OF A MUFFLER

DTIC
ELECTE
S
APR 1 0 1989
D
D

CHARLIE H. COOKE
KEVIN S. FANSLER

JANUARY 1989

Best Available Copy

APPROVED FOR PUBLIC RELEASE; DISTRIBUTION UNLIMITED.

U.S. ARMY LABORATORY COMMAND

BALLISTIC RESEARCH LABORATORY
ABERDEEN PROVING GROUND, MARYLAND

89 4 07 130

REPORT DOCUMENTATION PAGE

Form Approved
OMB No. 0704-0188

1a. REPORT SECURITY CLASSIFICATION UNCLASSIFIED	1b RESTRICTIVE MARKINGS
2a. SECURITY CLASSIFICATION AUTHORITY	3 DISTRIBUTION/AVAILABILITY OF REPORT
2b DECLASSIFICATION/DOWNGRADING SCHEDULE	Approved for public release; distribution unlimited.

4 PERFORMING ORGANIZATION REPORT NUMBER(S) BRL-MR-3735	5 MONITORING ORGANIZATION REPORT NUMBER(S)

6a. NAME OF PERFORMING ORGANIZATION U.S. Army Ballistic Research Laboratory	6b. OFFICE SYMBOL (If applicable) SLCBR-LF	7a NAME OF MONITORING ORGANIZATION
6c. ADDRESS (City, State, and ZIP Code) Aberdeen Proving Ground, MD 21005-5066		7b. ADDRESS (City, State, and ZIP Code)

8a. NAME OF FUNDING/SPONSORING ORGANIZATION U.S. Army Ballistic Research Laboratory	8b OFFICE SYMBOL (If applicable) SLCBR-DD-T	9 PROCUREMENT INSTRUMENT IDENTIFICATION NUMBER

8c. ADDRESS (City, State, and ZIP Code) Aberdeen Proving Ground, MD 21005-5066	10 SOURCE OF FUNDING NUMBERS			
	PROGRAM ELEMENT NO. 62618A	PROJECT NO. 1L1 62618AH80	TASK NO.	WORK UNIT ACCESSION NO.

11. TITLE (Include Security Classification)

Numerical Simulation and Modeling of a Muffler (U)

12. PERSONAL AUTHOR(S)
Cooke, Charlie H., and Fansler, Kevin S.

13a. TYPE OF REPORT Memorandum Report	13b TIME COVERED FROM _____ TO _____	14. DATE OF REPORT (Year, Month, Day) 1989 January	15. PAGE COUNT 26

16. SUPPLEMENTARY NOTATION

17.	COSATI CODES		18. SUBJECT TERMS (Continue on reverse if necessary and identify by block number)
FIELD	GROUP	SUB-GROUP	Gun Attenuators Unsteady Euler
19	04		Impulse Noise Computations,
20	04		Computational Fluid Dynamics

19. ABSTRACT (Continue on reverse if necessary and identify by block number)

The problem of attenuating the noise from weapons firing was studied, experimentally and numerically. As a possible method of attenuating the noise significantly, a silencer with no internal baffles was attached to the M242 cannon. The internal pressures at selected locations inside the muffler were measured. The near field overpressures outside the muffler at various polar angles were also measured. A numerical simulation of the flow through the muffler was performed, using Harten's shock capturing method to solve the Euler equations of ideal compressible flow. The numerical simulation yields a detailed picture of the flow field as displayed by the pressure and Mach contours. Pressure-time curves obtained at selected locations are compared with experimental data. There is good agreement except that the numerical simulation generates more vigorous oscillations with higher peak values. As an aid to understanding the early flow processes in the muffler and as a design tool requiring little computational effort, a one-dimensional analytical model was constructed.

20. DISTRIBUTION/AVAILABILITY OF ABSTRACT ☐ UNCLASSIFIED/UNLIMITED ☒ SAME AS RPT ☐ DTIC USERS	21 ABSTRACT SECURITY CLASSIFICATION UNCLASSIFIED	
22a. NAME OF RESPONSIBLE INDIVIDUAL Dr. Kevin S. Fansler	22b TELEPHONE (Include Area Code) 301-278-4365	22c. OFFICE SYMBOL SLCBR-LF-F

DD Form 1473, JUN 86   Previous editions are obsolete.   SECURITY CLASSIFICATION OF THIS PAGE

Acknowledgment

Accesion For		
NTIS CRA&I	☑	
DTIC TAB	☐	
Unannounced	☐	
Justification		
By		
Distribution /		
Availability Codes		
Dist	Avail and/or Special	
A-1		

Table of Contents

List of Figures

List of Tables

I. Introduction

The firing of gun weapons often generates objectionable levels of noise. Different methods or combinations of methods can be used to attenuate the noise. One possible response is to develop muzzle devices that attenuate the blast in all directions. These muzzle devices are referred to as noise attenuators, silencers, or mufflers and are sometimes used with small-caliber rifles and pistols. They suppress gun muzzle blast by reducing the rate of propellant energy being released from the exit hole.[1,2,3,4] No adequate model exists for the flow internal to the muffler; this flow is very complicated and, for the larger mufflers, is significantly modified by energy transfer of the propellant gases to the body of the muffler. In general, the muffling of the noise increases with the size of the muffling device; attenuation levels up to 40 dB have been claimed. However, the weapons producing the objectionable noise may be larger caliber guns, such as the 25 mm M242 automatic cannon. It is not practical to scale up the noise attenuators designed for small-caliber guns to the size required for the 25 mm cannon, as the added bulk could compromise system performance by making the larger weapon unwieldy. Although mufflers with many bore and chamber volumes have been investigated, work on smaller mufflers has been neglected because generally higher noise attenuation is desired than can be thus achieved.

The immediate objective of this study is to simulate a small muffler adequately by a particular numerical technique. The flow field inside the silencer during the firing cycle is simulated and then measured by experiment for validation of the scheme. A total variation diminishing (TVD) shock-capturing scheme is employed, with sufficient grid density to yield the necessary flow details.[5] Fluid property contours and pressure-time curves at selected locations are generated. Corresponding free-field blast overpressures and internal pressures within the muffler are obtained for comparison with the computational results. Guided by the results of the experiment and the simulation, a one-dimensional model for the peak energy efflux exiting the muffler projectile hole was developed. The peak energy efflux is the maximum rate of the sum of the propellant gas's kinetic energy and potential energy that passes through the muffler projectile hole. Results from the one-dimensional model are compared with those from the experiment and the simulation.

Comparisons of blast overpressure in this report will generally be given in terms of dB levels. The sound pressure level attenuation is

$$dB_{pk} = 20\log_{10}(P_2/P_1) \qquad (1)$$

Here, P_2 is the new value of peak overpressure and P_1 is the value of the reference peak overpressure.

---

[1] Fansler, K. S., and Schmidt, E. M., "The Relationship Between Interior Ballistics, Gun Exhaust Parameters and the Muzzle Blast Overpressure," AIAA Paper 82-0856, AIAA/ASME 3rd Joint Thermophysics, Fluids, Plasma and Heat Transfer Conference, St. Louis, MO, 7-11 June 1982.

[2] Heaps, C. W., Fansler, K. S., and Schmidt, E. M., "Computer Implementation of a Muzzle Blast Prediction Technique," ARBRL-MR-3443, U.S. Army Ballistic Research Laboratory, Aberdeen Proving Ground, Maryland, May 1985. (AD A158344)

[3] Fansler, K. S., "Dependence of Free Field Impulse on the Decay Time of Energy Efflux for a Jet Flow," *Proceedings of the 56th Shock and Vibration Symposium*, U. S. Naval Postgraduate School, Monterey, CA, 22-24 October 1985.

[4] Smith, F., "A Theoretical Model of the Blast from Stationary and Moving Guns," *First International Symposium on Ballistics*, Orlando, Florida, 13-15 November 1974.

[5] Harten, A., "High Resolution Schemes for Hyperbolic Conservation Laws," *Journal of Computational Physics*, Vol. 49, 1983, pp. 357-393.

II. Theory and Numerical Simulation Technique

1. Prediction of Blast Overpressure

Investigators have found it difficult to develop a comprehensive theory for noise suppression in mufflers. Usually, they have first examined the theoretical flow details within the silencer and then proceeded to develop prediction methods for the overpressure around the gun. However, with the exit properties of the weapon assumed known, the blast field overpressure can be predicted in a quite simple way.[1,2,3] A method is used whose theoretical foundations depend upon blast wave scaling theory for variable energy deposition rates, coupled with the theory of blast waves generated by asymmetrically initiated charges.[4] More precisely, these particular scaling relations were developed from the assumption that a primary parameter for the gun blast phenomena is the rate of energy deposit into the ambient air. To minimize the peak energy deposition rate from the weapon and thereby the peak overpressure at a point in the field, the model shows that the exit hole diameter for the silencer, the maximum exit pressure from the silencer, and the exit propellant gas velocity should all be minimized.

2. Overview of the Numerical Scheme

The Harten scheme[5] is a TVD, second-order accurate, and upwind-biased method for solving the Euler equations of compressible flow in one dimension. The concept of operator splitting, placed on an analytical foundation by Strang,[6] permits application to higher dimensions and axisymmetric flow problems. Strang's work has been extended to allow the incorporation of source terms into the splitting, while at the same time preserving the second-order accuracy of the method.[7] The resulting shock-capturing algorithm is well-documented,[8] with clarifying background material provided.[5]

3. Cannon and Muffler Description

The simulation is performed for the 25mm cannon with the silencer attached. Figure 1 shows a schematic of the muzzle device tested. The inside cylinder of the muffler is threaded to permit varying the internal length of the muffler. For this experiment, the internal length of the silencer chamber is 7.7 calibers; the exit hole of the silencer is 1.14 calibers in diameter; the exit wall thickness is 0.7 caliber; and the computational domain extends approximately 1.7 calibers downstream of the silencer exit. The cannon's bore length is 80 calibers. Two gages were inserted into the muffler to obtain pressures for comparison with results from the numerical simulation. The free-field blast overpressure is measured using an array of static transducers located in an arc with its plane vertical and at a distance

[6] Strang, G., "On The Construction and Comparison of Difference Schemes," *SIAM Journal of Numerical Analysis*, Vol. 5, No. 3, Sept. 1968, pp. 506-517.

[7] Cooke, C. H., "On Operator Splitting for Unsteady Boundary Value Problems," *Journal of Computational Physics*, in press.

[8] Cooke, C. H., "On Operator Splitting of The Euler Equations Consistent with Harten's TVD Scheme," *Numerical Methods for Partial Differential Equations*, John Wiley and Sons, Inc, New York, 1985.

of 50 calibers from the projectile exit hole. At the time equal to zero, the back of the projectile exits the muzzle. All time before the projectile exits the muzzle is given as a negative quantity.

4. Precursor Flow and Blast Wave Initialization

When the gun is fired, the inbore projectile pushes a column of air with a shock front and constitutes the precursor flow from the barrel. For the numerical simulation it is thought sufficient to assume that the precursor wave inbore is generated by a piston traveling at a constant rate. This results in a pressure of 1.73 MPa and Mach number of 1.92 with, of course, the inbore precursor's fluid velocity being equal to the projectile velocity. The projectile is simulated by a cylinder three calibers long. The gasdynamic quantities behind the projectile were obtained using Lagrangian interior ballistics and the experimentally measured pressure at projectile exit from the cannon muzzle. A one-dimensional Harten code was used to calculate the flow inbore. Upon projectile exit, flow values at the muzzle were:

$$p_e = 33.4 \text{ MPa}$$
$$V_e = 1050 \text{ m/s}$$
$$M_e = 1.52$$

III. Numerical Results and Comparisons with Experiment

Flow in the silencer was simulated on a VAX-8600 computer system. Initially, a grid density of 41 points per caliber was employed. Results shown in this report were obtained, for the most part, on this grid. For a feasibility study of calculations on finer grids, a much larger computer is necessary. However, a short run on an 81-points-per-caliber grid was accomplished, to assess the numerical accuracy. Although some improvement appears to result, the pressure trends were much the same.

As mentioned earlier, the precursor flow for the numerical simulation scheme is treated initially as a uniform mass of gas having the velocity of the projectile, which determines its pressure and density. Figure 2 shows the pressure contours just before the precursor shock wave hits the front baffle. The time as given at the top of the plot is -150 μs. The position of the inward-facing shock is clearly delineated. The shape of the shock front is a slightly curved line; this curvature is attributed to reflection of the waves from the cylinder walls. Figure 3 shows the pressure contours just after the front of the precursor shock wave impinges on the front baffle and is reflected. These pressure contours occur at -87 μs.

Figure 4 shows contours of pressure immediately after the shock wave, which is driven by the propellant gas, reaches the front baffle. Figure 5 shows Mach contours; the presence of the projectile slows the progress of the inward-facing shock at the positions close to the axis. The Mach contours also delineate the shear layers in the flow.

3

In the experimental setup, internal pressures were obtained at $r = 0.5$ caliber on the cylinder side and at $r = 1.5$ caliber on the exit baffle. Here, x is the distance forward from the internal rear face of the muzzle plate and r is the radial position from the axis. Figure 6 shows the comparisons between experimental and numerical overpressures obtained at position $x = 0.5$ caliber on the side of the cylinder. Good agreement between experiment and simulation is obtained, for the times from zero to 0.4 ms. Agreement is encouraging until approximately 0.7 ms; after this time the simulation yields more vigorous pressure oscillations. The large pressure jump at 0.5 ms occurs when the reflected wave from the front baffle reaches this position. Figure 7 shows the comparison between experiment and simulation for the front baffle. Comparison could not be made near 0.4 ms because experimental data were not received correctly, probably because of severe signal cable movement. The reflected overpressure for the precursor wave is slightly higher for the experiment, due possibly to propellant gas blow-by around the projectile while inbore. The simulation gives much more pronounced peaks; these peaks have a frequency that is approximately what one might expect for waves traveling from the cylinder walls to the center and back. For later times, the simulated values are clearly greater than the experimental values. This disagreement may occur partly because the output of the pressure transducers is reduced by prolonged exposure to the high-temperature propellant gas. Also, almost one-tenth of the propellant's internal energy is transferred to the muffler in the form of heat energy, thus lowering the pressure for the longer times. Yet another possibility is that the inviscid method may not model the separated flow at the exit hole correctly. The simulated region of recirculation at the hole may be too large, thus restricting the flow from the muffler. Figure 8 shows the variations in the pressure at two radial positions on the baffle as obtained by simulation. The initial peak values differ drastically; waves traveling in the radial direction could generate such differences in peak values.

The energy efflux from the muffler is calculated as part of the numerical simulation. A log function of an energy efflux ratio is shown in Figure 9, the ratio consisting of the temporal energy efflux from the exit hole of the muffler divided by the peak energy efflux from the gun muzzle. For the prediction method which uses the scaling approach,[2,3] the scale of the muzzle blast is determined by this peak energy efflux from the muzzle. It is assumed that the energy efflux values from the muffler would also determine the scale of the associated blast wave although the peak value might not determine the scale, especially if the duration of the wave were very short compared to the exhaust time of the muffler. The greatest values of the function plotted in Figure 9 represents an approximation of the attenuation in dB's expected for the muffler compared to the the bare muzzle value. At first, the value of the function represents the energy efflux from the precursor wave. The blast wave generated by the propellant gas reaches the exit baffle between 0.1 and 0.2 ms. The first maximum values are associated with the reflection of the initial shock wave at the exit baffle. The general upward movement of the energy efflux values with time occurs because the rate of mass flow from the muzzle into the muffler exceeds the mass flow rate from the projectile hole of the muffler, thus bringing the general pressure level up everywhere in the muffler. However, the amount of upward movement from the initial reflected values is small. Thus, longer cylinders or inlet lengths should result in very little improvement in noise attenuation as the sound levels would then depend upon the value for the reflected pressure from the baffle. Experiment confirms this as shown in Figure 10. There is little difference in attenuation values between the shortest and

4

the longest configurations. The shortest muffler would be the most attractive from the standpoint of weight.

IV.   One-Dimensional Model and Comparisons

The length of the silencer compared to its width suggests modeling the early flow processes by one-dimensional gas dynamics. The simulation shows that the shock front for the blast wave in the silencer forms an almost straight line. Moreover, the early processes for the simulated flow resemble the start-up processes of one-dimensional flow. The model is most easily explained for the case of a blast wave exiting the bore in the absence of a projectile. As the gas exits the muzzle into the silencer, it is free to expand to supersonic conditions. An inward-facing shock immediately forms, which raises the pressure above ambient. The shock front of this higher pressure gas travels toward the baffle front and is reflected toward the muzzle. The gas behind the reflected shock is then free to exit the front baffle's projectile hole at the sonic velocity and with a stagnation pressure that depends on the strengths of the shocks that have passed through the propellant gas. This phase can be readily modeled employing one-dimensional gasdynamics. Initial conditions inside the muffler are assumed to account for the air pushed out of the bore ahead of the projectile.

Comparisons are made with the one-dimensional model at early times after the projectile leaves the muzzle, thereby releasing the propellant gas to flow into the muffler. The one-dimensional model would not be expected to give as good results for propellant flow as for the precursor flow, unless the precursor flow is modeled well. The complicated precursor flow precedes the propellant flow, whereas the precursor flow empties into ambient air. For the propellant flow, we make the rough approximation that the air in the barrel is isentropically compressed and not moving. The propellant gas is then assumed to empty into the muffler with no resident projectile; i.e., no modeling is attempted of the projectile's interaction with the propellant gas flow.

In Figure 11 the one-dimensional processes are schematically indicated by means of an x-t diagram, with the gas exhausting through the exit hole modeled as a porous-wall boundary condition. Here, it is seen that the reflected shock front travels back toward the muzzle and impinges on the contact surface. The contact surface velocity is reduced to a much smaller value and shock waves travel away from the interacted contact surface in both directions. The shock wave reflected from the contact surface that impinges upon the wall further increases the wall pressure. The resulting shock wave traveling away from the contact surface and the wall interacts with the inward-facing shock, generating a shock traveling to the left and a rarefaction wave traveling back toward the wall. The unfilled circles denotes the trajectory of the contact surface that stems from the interaction of these two shocks. The second reflected shock coming off the baffle interacts with the contact surface denoted by the filled circles. The resulting left moving shock then interacts with the right moving expansion wave referred to before. The resulting contact surface trajectory is delineated by the filled squares. Essentially, as these shocks travel back toward the muzzle and interact, increasing regions behind the shocks have a reverse flow. The region for high-speed right moving flow retreats as these shocks traverse the propellant gas.

5

Figure 12 shows the pressure contours obtained by simulation at 350 micro-seconds. The shock has traveled back to a position close to the muzzle. Comparison with Figure 11 shows that extrapolation from the wave diagram to a time of 350 micro-seconds yields a shock position further from the muzzle. The inward-facing shock positions of the two models do not agree well for smaller times. This occurs partly because the flow nearer the cylinder wall goes through an oblique shock and then propagates pressure waves down toward the axis, thus retarding the speed of the inward-facing shock near the axis. Also, the exit conditions for the simulated two-dimensional flow are changing to lower pressure and velocity values, which would slow the shock speed as compared to the one-dimensional model. The presence of the projectile also retards the movement of the inward-facing shock. In the two-dimensional case, the shocks are curved, and from Crocco's theorem, the region between the inward-facing shock and the exit baffle should be filled with recirculating flows, which indeed it is, as seen from the velocity vector plot of Figure 13.

Table 1 below summarizes and compares the peak overpressures obtained on the exit baffle of the silencer.

Table 1. Reflected Overpressure (MPa) on Exit Baffle

Phase	Experiment	Simulation	1-D Model
Precursor	2.0	1.5	2.3
Propellant(1.5 cal)	11.4	17.0	26.0
Propellant(0.8 cal)		37.0	

The precursor experimental values are in fair agreement with simulation and the one-dimensional model but the propellant simulated value is grossly higher at the point 0.8 caliber from the axis. If it is assumed that the propellant gas exits the muzzle into the muffler with atmospheric pressure, the 1-D model yields approximately 19 MPa. With both assumptions, the 1-D model gives values that are too high. Nevertheless, the model can give guidance about the general levels of pressure to expect on the baffle in the inlet chamber of a muffler.

The one-dimensional model can also explain why the blast from some mufflers is attenuated more when the weapon is fired on automatic mode. The one-dimensional model predicts lower reflected pressures when hot gases initially fill a muffler at normal atmospheric conditions. If the minimum length requirement is met for the hot gas conditions, the muffler will produce a greater attenuation than for a cool gas. If not, the maximum pressure inside the chamber will exceed the reflected overpressure.

Comparisons can also be made for earlier times. Figure 2 shows the pressure contours corresponding to a time before the shock hits the front baffle. The maximum pressure shown here is 662 kPa. The one-dimensional model yields 560 kPa, a significantly lower value. However, the one-dimensional model assumes that the flow passes through a normal inward-facing shock, whereas the numerical simulation shows some of the flow passing through a weaker oblique shock.

6

V. Summary and Conclusions

A numerical simulation scheme was utilized to compute the flow inside the muffler configuration that had no internal baffles and the shortest internal length. These results were compared with pressure histories recorded 0.5 caliber from the rear internal disk on the muffler cylinder wall and 1.5 caliber from the axis on the inside surface of the front baffle. The numerical results for the cylinder agree well for the first part of the flow process on the cylinder but show larger variations in pressure than the experimental data. For the front baffle, simulation results show large oscillations compared to experiment. These excessive oscillation levels might be attenuated by taking viscosity into account. At both probes for the later times, the simulated pressures are larger. This indicates that the separator flow at the projectile hole is not well modeled by the inviscid scheme. To test these conjectures and in an attempt to obtain more accurate results, a viscous simulation scheme will be developed that includes viscous terms.

A one-dimensional model for the flow was also developed, to a crude level of sophistication. The one-dimensional model yields high pressure values compared to experiment. Nevertheless, the 1-D model should prove useful for designing the baffle in the inlet chamber of mufflers. It also aids in our understanding of why the internal lengths did not appear to be a significant parameter for the prediction of free-field blast overpressure. As long as the muffler has a minimum internal length, the propellant gas exhausting from the barrel will not raise the baffle exit pressure high enough to produce a significantly higher energy efflux than is produced by the initial pressures resulting from the shock first reflected from the front baffle.
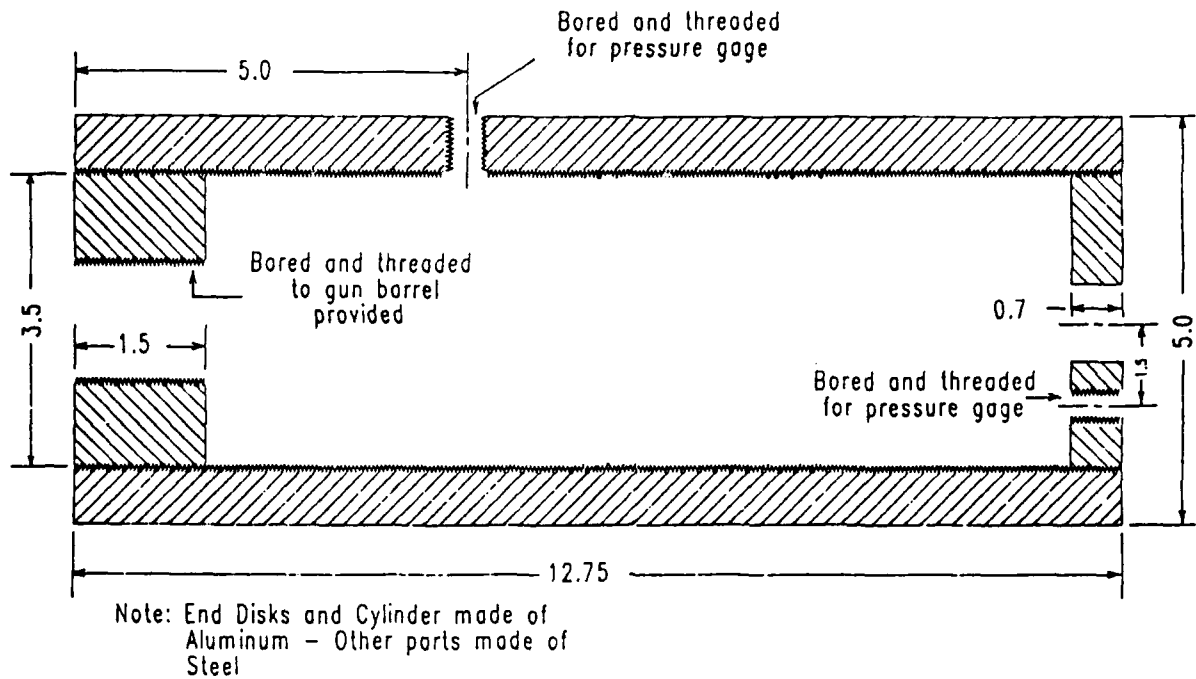
Figure 1. Schematic of BRL Muffler.
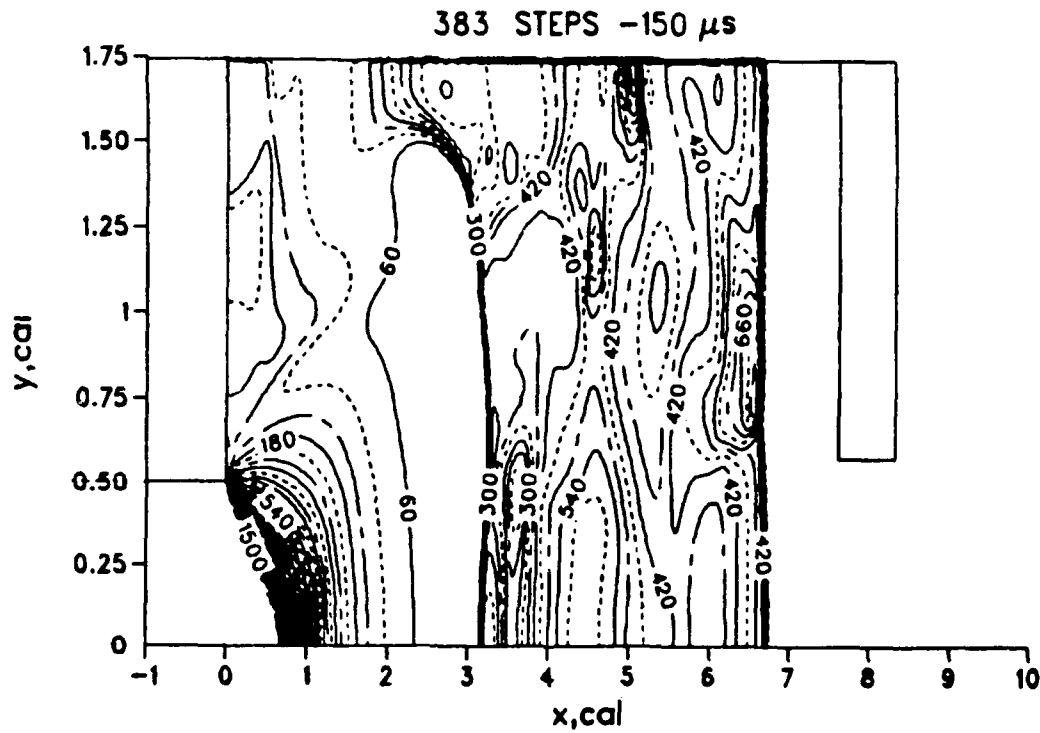
Figure 2. Pressure Contours (kPa) Obtained by Numerical Simulation of Precursor Flow.

8
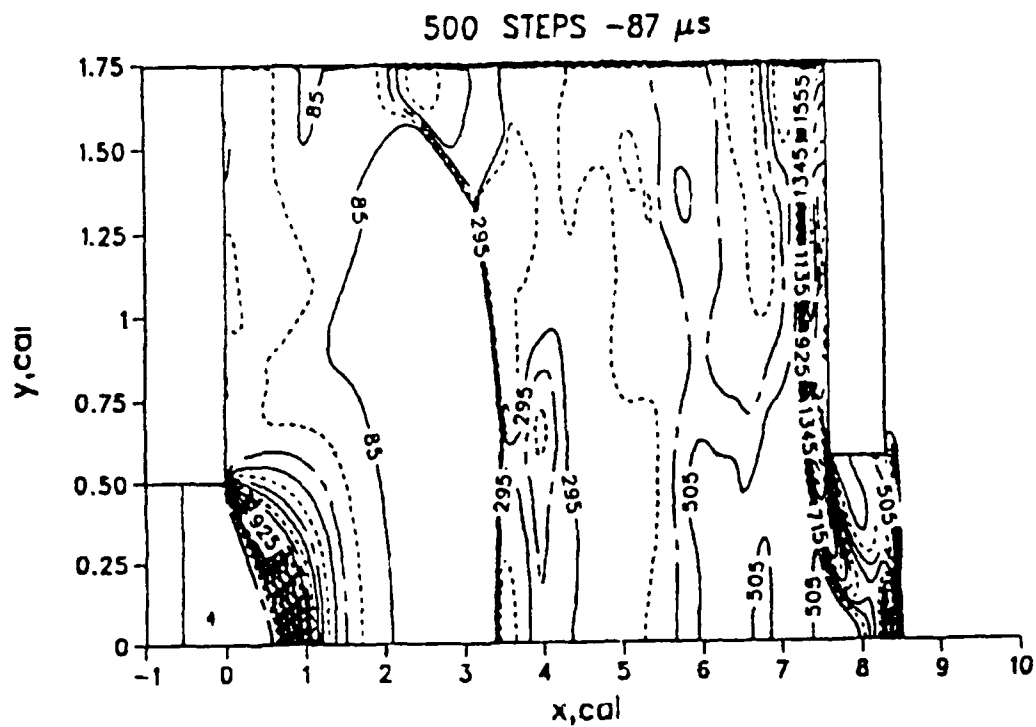
Figure 3. Pressure Contours of Precursor Flow at the Time When the Shock Front Hits the Wall.
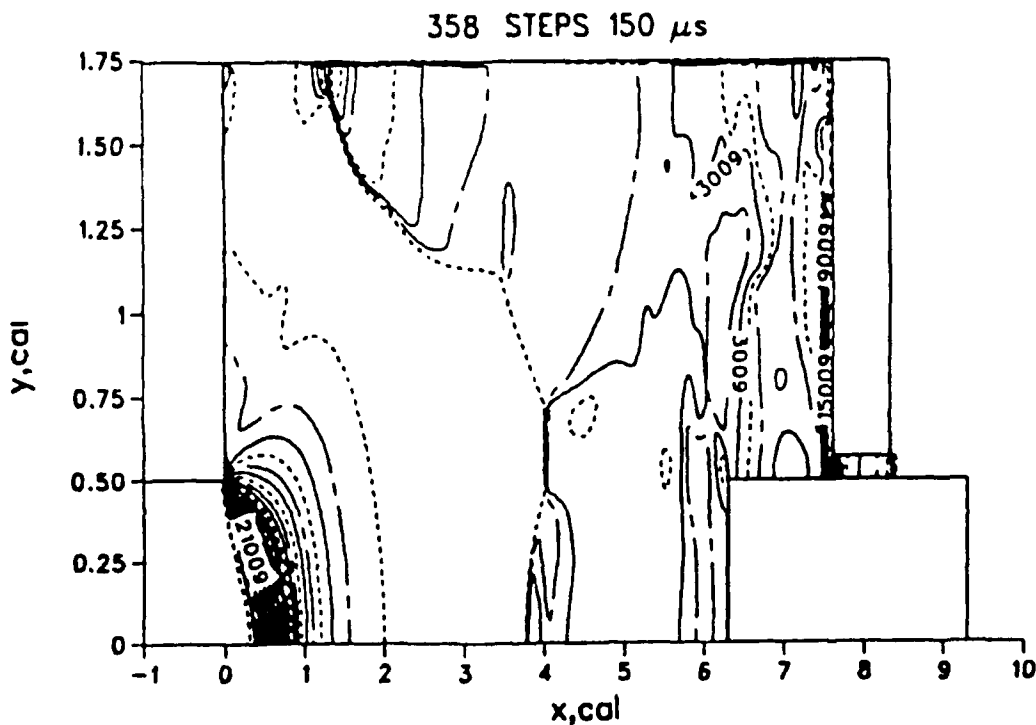
Figure 4. Contours of Propellant Flow at the Time When the Shock Front Hits the Wall. Pressure Contours (kPa).

358 STEPS 150 µs
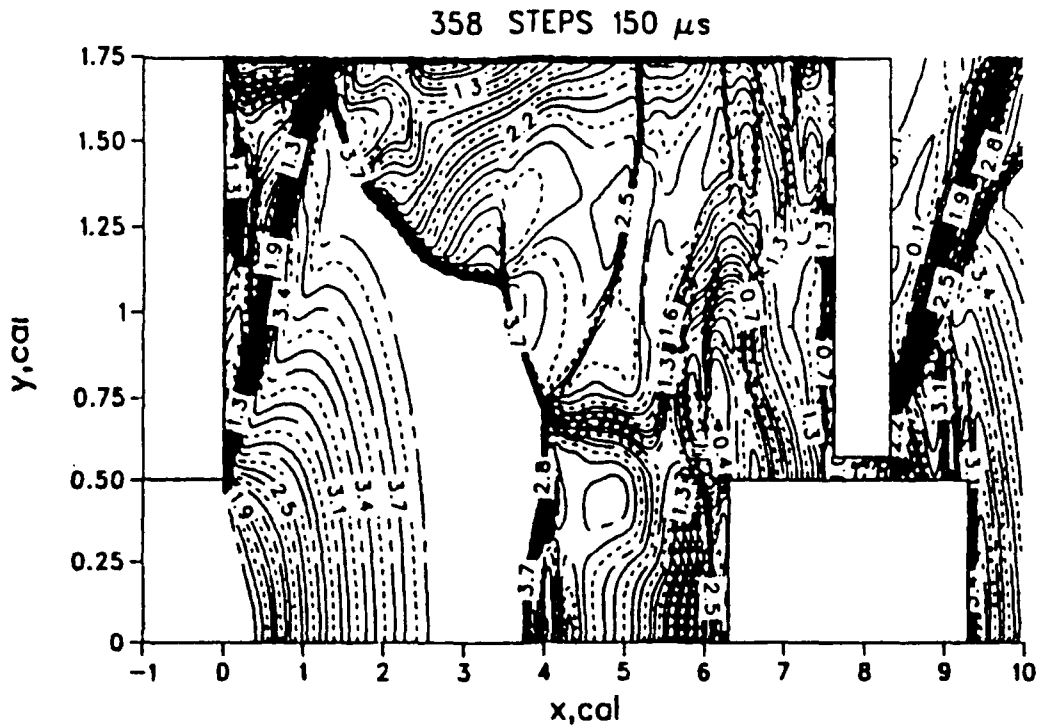
Figure 5. Contours of Propellant Flow at the Time When the Shock Front Hits the Wall. Mach Contours.
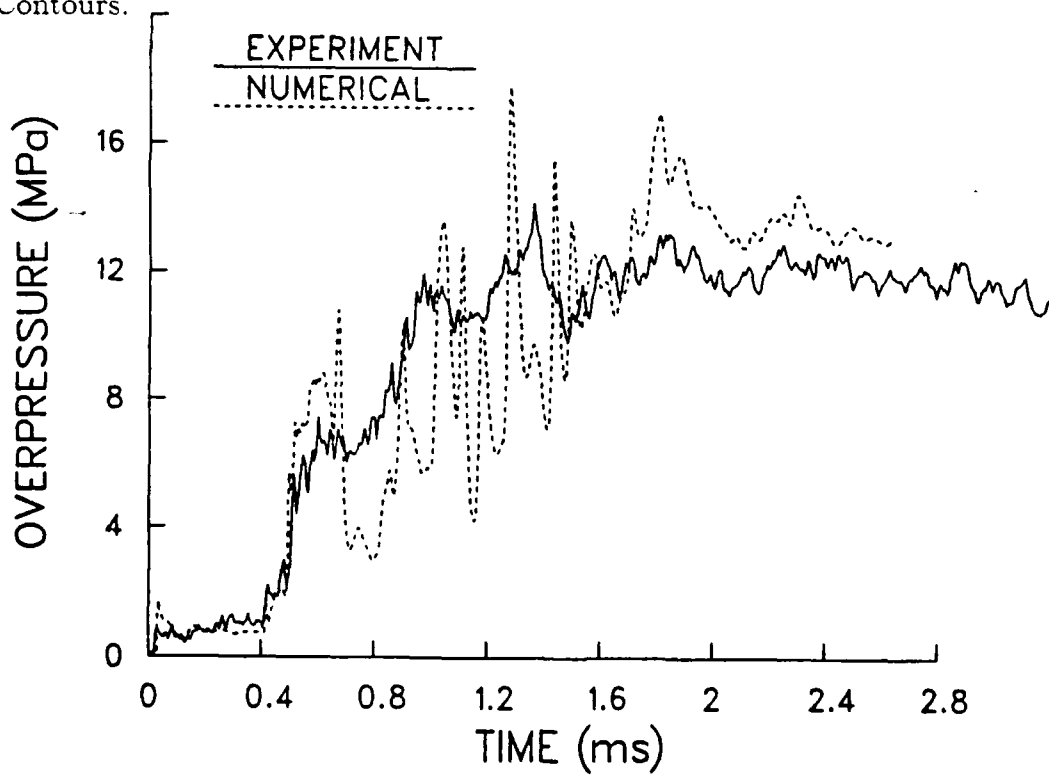
Figure 6. Comparison of Experimental and Simulation Pressure at the Cylinder Wall 0.5 Caliber from the Rear Muffler Wall.
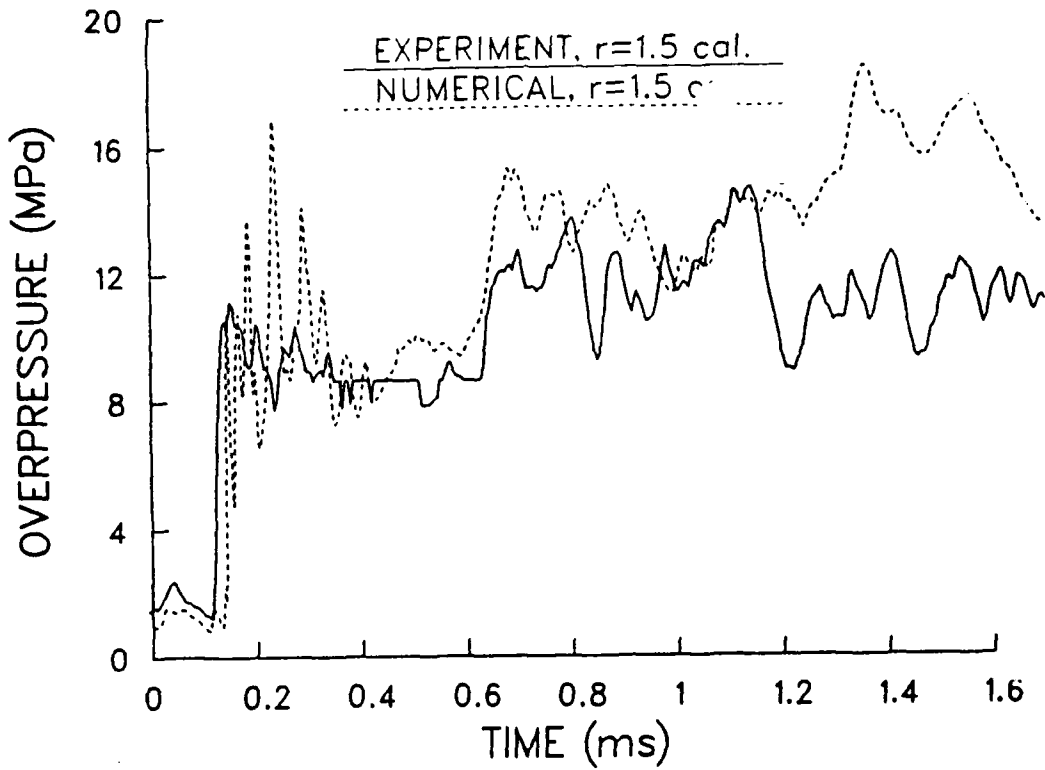
Figure 7. Pressure Comparisons at the Front Baffle. Numerical Simulation and Experiment at r = 1.5 Caliber.
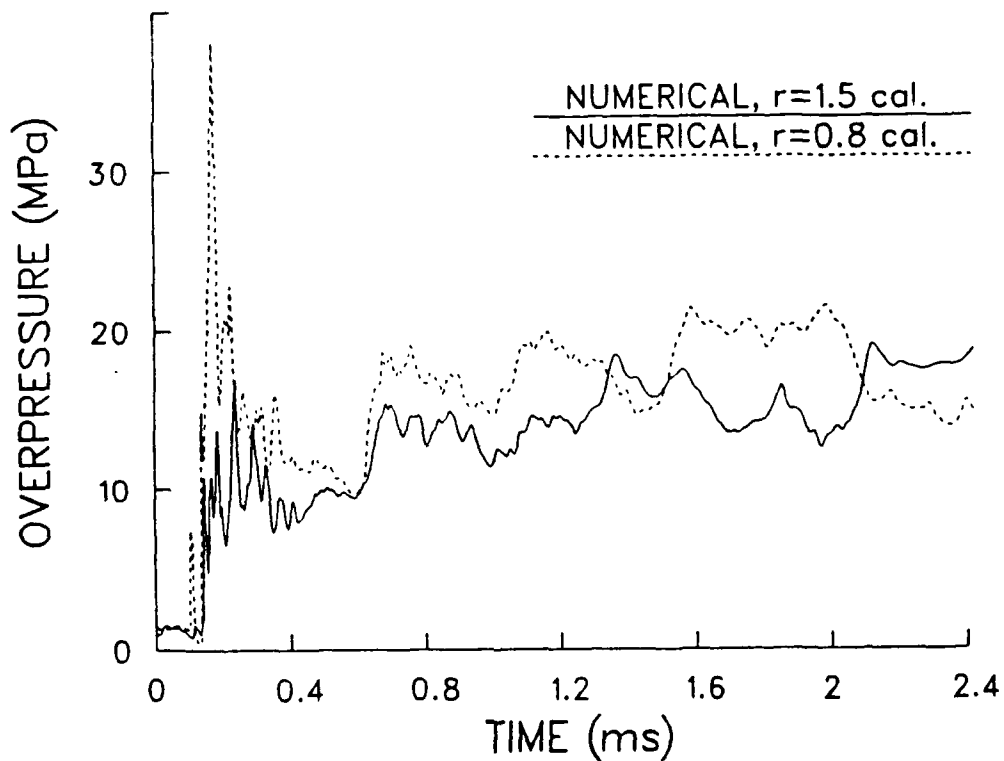
Figure 8. Pressure Comparisons at the Front Baffle. Numerical Simulations at r = 1.5 and r = 0.8 Caliber.
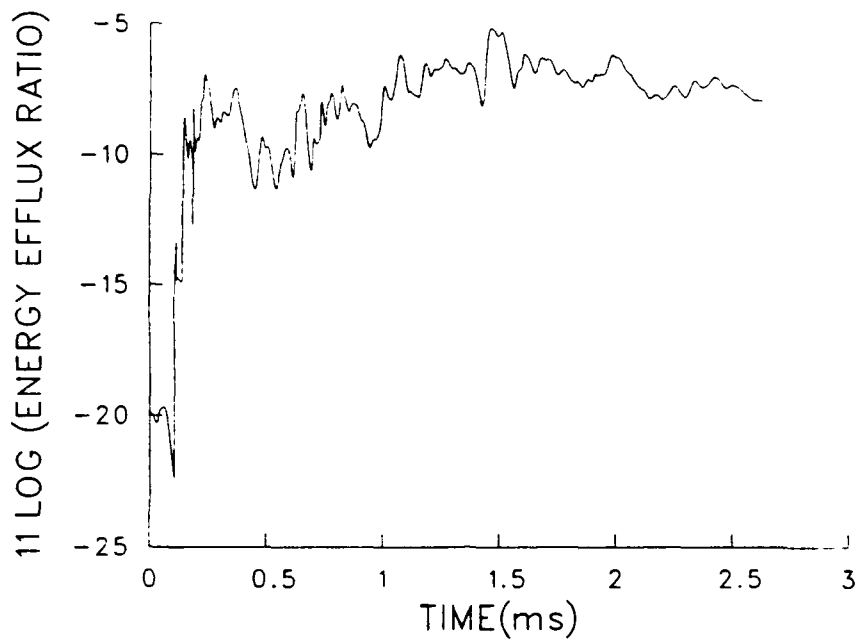
Figure 9. Energy Efflux from Muffler as a Function of Time.
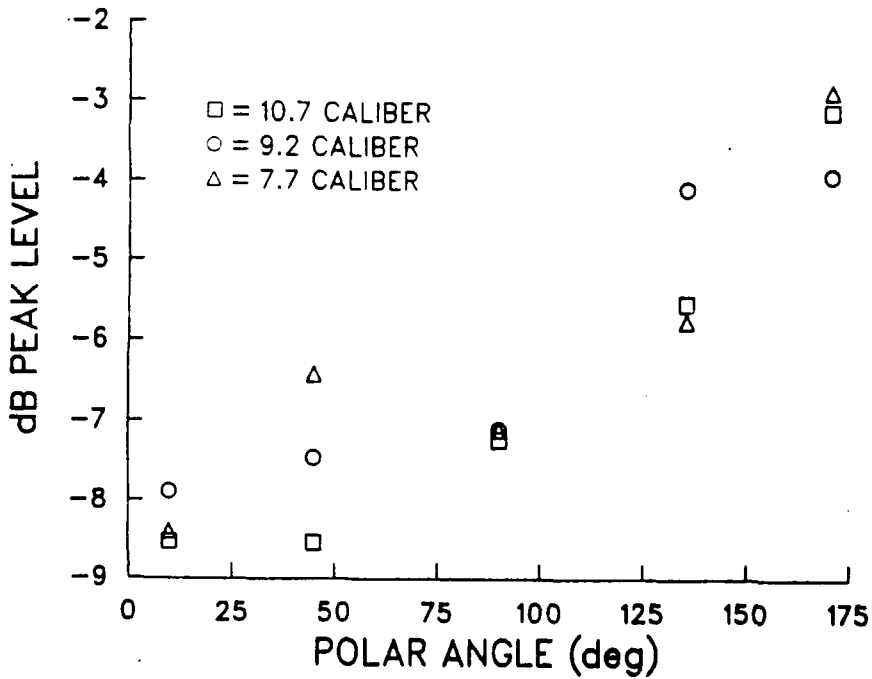
Figure 10. Peak Sound Levels (Referred to Bare Muzzle Values) for Smallest Muffler with Different Internal Lengths versus Polar Angle from the Firing Direction.

12

Figure 11. The Distance versus Time Diagram for the One-Dimensional Model of the Flow in the Muffler.

Figure 12. Flowfield at 350 microseconds. Contours of Pressure.

13
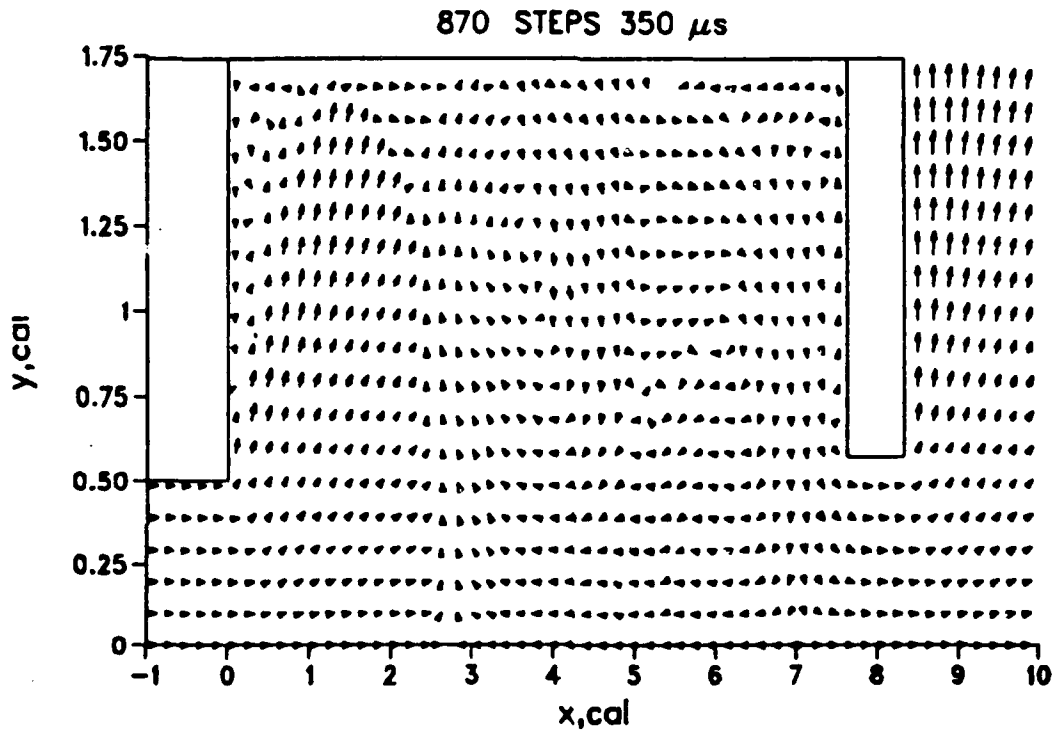
Figure 13. Flowfield at 350 microseconds. Velocity Vector Plot.

14

References

1. Fansler, K. S., and Schmidt, E. M., "The Relationship Between Interior Ballistics, Gun Exhaust Parameters and the Muzzle Blast Overpressure." AIAA Paper 82-0856, AIAA/ASME 3rd Joint Thermophysics, Fluids, Plasma and Heat Transfer Conference, St. Louis, MO, 7-11 June 1982.

2. Heaps, C. W., Fansler, K. S., and Schmidt, E. M., "Computer Implementation of a Muzzle Blast Prediction Technique," ARBRL-MR-3443, U.S. Army Ballistic Research Laboratory, Aberdeen Proving Ground, Maryland, May 1985. (AD A158344)

3. Fansler, K. S., "Dependence of Free Field Impulse on the Decay Time of Energy Efflux for a Jet Flow," *Proceedings of the 56th Shock and Vibration Symposium*, U. S. Naval Postgraduate School, Monterey, CA, 22-24 October 1985.

4. Smith, F., "A Theoretical Model of the Blast from Stationary and Moving Guns," *First International Symposium on Ballistics*, Orlando, Florida, 13-15 November 1974.

5. Harten, A., "High Resolution Schemes for Hyperbolic Conservation Laws," *Journal of Computational Physics*. Vol. 49. 1983, pp. 357-393.

6. Strang, G., "On The Construction and Comparison of Difference Schemes," *SIAM Journal of Numerical Analysis*, Vol. 5, No. 3, Sept. 1968, pp. 506-517.

7. Cooke, C. H., "On Operator Splitting for Unsteady Boundary Value Problems." *Journal of Computational Physics*, in press.

8. Cooke, C. H., "On Operator Splitting of The Euler Equations Consistent with Harten's TVD Scheme." *Numerical Methods for Partial Differential Equations*, John Wiley and Sons, Inc., New York. 1985.

DISTRIBUTION LIST

No. Copies	Organization	No. Copies	Organization

12	Administrator
	Defense Technical
	   Information Center
	ATTN: DTIC-DDA
	Cameron Station,
	Alexandria, VA 22304-6145
		1	Commander
			US Army Communications -
			   Electronics Command
			ATTN: AMSEL-ED
			Fort Monmouth, NJ 07703-5022

1	HQDA SARD-TR Washington, DC 20310-0001	1	Commander US Army Laboratory Command ATTN: AMSLC-DL Adelphi, MD 20783-1145
1	Commander US Army Materiel Command ATTN: AMCDRA-ST 5001 Eisenhower Avenue Alexandria, VA 22333-0001	2	Commander US Army Missile Command ATTN: AMSMI-RD, Dr. Bill Walker ATTN: AMSMI-AS Redstone Arsenal, AL 35898-5000
1	Commander US Army Armament, Munitions and Chemical Command ATTN: AMSMC-LEP-L Rock Island, IL 61299	1	Director US Army Missile & Space Intelligence Center ATTN: AIAMS-YDL Redstone Arsenal, AL 35898-5000
1	Commander US Army Armament, Munitions and Chemical Command ATTN: SMCAR-ESP-L Rock Island, IL 61299-5000	11	Commander US Army Armament RD&E Center ATTN: SMCAR-MSI (2 cys) ATTN: SMCAR-FS, Dr. Davidson ATTN: SMCAR-FSF, Mr. Ambrosini ATTN: SMCAR-FSA, Mr. Wrenn

1	Director
	US Army TRADOC
	   Analysis Command
	ATTN: ATAA-SL
	White Sands Missile Range
	NM 88002-5502
			ATTN: SMCAR-CC, Mr. Hirshman
			ATTN: SMCAR-CCH, Mr. Moore
			ATTN: SMCAR-CCL, Mr. Gehbauer
			   E. Seeling
			   J. Donham
			ATTN: SMCAR-LCW, M. Salsbury
			Picatinny Arsenal, NJ 07801-5000

1	Director US Army Aviation Research and Technology Activity Ames Research Center Moffett Field, CA 94035-1099		

DISTRIBUTION LIST

No. Copies	Organization	No. Copies	Organization
3	Commander US Army Tank Automotive Command ATTN: AMSTA-TSL ATTN: AMCPM-BFVS ATTN: AMSTA-DI Warren, MI 48397-5000	1	AFWL/SUL Kirtland AFB. NM 87117-5800
		2	Air Force Armament Laboratory ATTN: AFATL/DLODL Tech Lib Eglin AFB, FL 32542-5000
1	Commander US Army Research Office P.O. Box 12211 Research Triangle Park, NC 27709	1	Commandant USAFAS Fort Sill. OK 73503-5600
1	Commander US Army Aviation Systems Command ATTN: AMSAV-DACL 4300 Goodfellow Blvd St. Louis. MO 63120-1798	7	Director Benet Weapons Laboratory Armament RD&E Center US Army AMCCOM ATTN: SMCAR-CCB. J. Bendick T. Simkins ATTN: SMCAR-LDB-D, J. Zweig ATTN: SMCAR-CCB-DS, P. Vottis ATTN: SMCAR-CCB-RA. G. Carofano ATTN: SMCAR-CCB-RA ATTN: SMCAR-LCB-TL Watervliet, NY 12189-4050
1	Commander US Naval Air Systems Command ATTN: AIR-604 Washington. DC 20360		
2	Commander Armament RD&E Center US Army AMCCOM ATTN: SMCAR-TDC Picatinny Arsenal. NJ 07806-5000	3	Commander US Army Watervliet Arsenal ATTN: SMCWV-QAR, T. McCloskey ATTN: SMCWV-ODW, T. Fitzpatrick ATTN: SMCWV-ODP, G. Yarter Watervliet, NY 12189
2	Commandant US Army Infantry School ATTN: ATSH-CD-CSO-OR ATTN: ATSH-IV-SD. R. Gorday Fort Benning, GA 31905-5660	2	President US Army Armor & Engineer Board ATTN: ATZK-AE-PD, Mr. A. Pomey Fort Knox, KY 40121
1	Commander ATTN: AEAGC-ATC-TS, P. Minton USAREUR. Grafenwohr, FRG APO. NY 09114		

DISTRIBUTION LIST

No. Copies	Organization	No. Copies	Organization

2	Commander
	Tank Main Armament Systems
	ATTN: AMCPM-TMA,
	    R. Billington
	Dover, NJ 07801-5001
		2	Commander
			Naval Surface Weapons Center
			ATTN: 6X
			    J. Yagla
			    G. Moore
			Dahlgren, VA 22448

1	Commander US Army Armor Center & School ATTN: ATSB-SMT, Maj Newlin Fort Knox, KY 40121	1	Commander Naval Weapons Center ATTN: K. Schadow Code 3892 China Lake, CA 93555
1	Commander U. S. Naval Training Center ATTN: AMCPM-TND-CTC, LTC Overstreet Orlando, FL 32813-7100	1	Commander Naval Surface Weapons Center ATTN: Code 730 Silver Spring, MD 20910

1	Department of the Army
	Construction Engineering
	    Research Laboratory
	ATTN: CERL-SOI,
	    P. Schomer
	P. O. Box 4000
	Champaign, IL 61820
		1	Director
			NASA Scientific & Technical
			    Information Facility
			ATTN: SAK/DL
			P. O. Box 8757
			Baltimore/Washington
			International Airport, MD 21240

1	Commander AMC-FAST Office ATTN: AMSLC-SA, R. Rogolski Fort Belvoir, VA 22060-5606	1	Honeywell Inc ATTN: R. Gartner 10400 Yellow Circle Drive Minnetonka, MN 55343

1	Commander
	Naval Sea Systems Command
	ATTN: 003
	Washington, DC 20362
		3	Honeywell Inc
			ATTN: MS MN 112190,
			    G. Stilley
			ATTN: MS MN 50-2060,
			    T. Melanger
			    S. Langley

1	Commander Naval Weapons Center ATTN: Code 3433, Tech Lib China Lake, CA 93555		600 Second Street, Northeast Hopkins, MN 55343

DISTRIBUTION LIST

No. Copies	Organization	No. Copies	Organization
1	Honeywell Ordnance ATTN: Craig Sletto Mail Stop 111443 23100 Sugarbush Road Elk River, MN 55330	1	Olin Corporation ATTN: L.A. Mason 707 Berkshire Blvd East Alton, IL 62024
1	S & D Dynamics, Inc. ATTN: R. Becker 2151 W. Hillsboro Blvd, No. 210 Deerfield Beach, FL 33442-1266	1	Aerospace Corporation ATTN: G. Widhopf Bldg. D8 M4/965 P. O. Box 92957 Los Angeles, CA 90009
1	AAI Corporation ATTN: J. Herbert P.O. Box 6767 Baltimore MD 21204	1	General Electric Armament & Electric Systems ATTN: R. Whyte Lakeside Avenue Burlington, VT 05401
1	AAI Corporation ATTN: T. Stasney P. O. Box 126 Cockeysville, MD 21030	1	Director Sandia National Laboratory ATTN: Aerodynamics Dept Org 5620, R. Maydew Albuquerque, NM 87115
3	Aerojet Ordnance Co ATTN: W. Wolterman S. Rush A. Flatau 2521 Michelle Drive Tustin, CA 92680	1	Franklin Institute ATTN: Tech Library Race & 20th Streets Philadelphia, PA 19103
1	Princeton Scientific Instruments, Inc ATTN: John Lowrance P.O. Box 252 Kingston, NJ 08528	1	Director Applied Physics Laboratory The Johns Hopkins University Johns Hopkins Road Laurel, MD 20707
2	United Technologies/Chemical Systems ATTN: R. MacLaren A. Holzman P. O. Box 50015 San Jose, CA 95150-0015	2	Loral Corporation ATTN: S. Schmotolocha B. Axely 300 N. Halstead St. P. O. Box 7101 Pasadena, CA 91109

20

DISTRIBUTION LIST

No. Copies	Organization	No. Copies	Organization
1	Martin Marietta Aerospace ATTN: A. Culotta P. O. Box 5837 Orlando, FL 32805		<u>Aberdeen Proving Ground</u>
3	McDonnell Douglas Helicopter Co. ATTN: J. Johnsen D. Van Osteen R. Waterfield Bldg 543 Mail Station D216 500 E. McDowell Rd. Mesa, AZ 85205		Director, USAMSAA ATTN: AMXSY-D, Mr. W. Brooks Mr. B. Siegel Mr. R. Conroy ATTN: AMXSY-MP, H. Cohen
1	FMC Corporation Northern Ordnance Division ATTN: S. Langlie 4800 East River Road Minneapolis MN 55421		Commander, USACSTA ATTN: STECS-AV-T, Mr. W. Swank ATTN: STECS-AS-LA, M. Maule
1	Old Dominion University Mathematics Department ATTN: Dr. Charlie Cooke Norfolk, VA 23508		Commander, USATECOM ATTN: AMSTE-TE-R Mr. Keele ATTN: AMSTE-TO-F Commander, CRDEC, AMCCOM ATTN: SMCCR-RSP-A ATTN: SMCCR-MU ATTN: SMCCR-SPS-IL
			Director, USAHEL ATTN: G. Garinther J. Kalb

21

USER EVALUATION SHEET/CHANGE OF ADDRESS

This laboratory undertakes a continuing effort to improve the quality of the reports it publishes. Your comments/answers below will aid us in our efforts.

1. Does this report satisfy a need? (Comment on purpose, related project, or other area of interest for which the report will be used.) _____
_____
_____

2. How, specifically, is the report being used? (Information source, design data, procedure, source of ideas, etc.) _____
_____
_____

3. Has the information in this report led to any quantitative savings as far as man-hours or dollars saved, operating costs avoided, or efficiencies achieved, etc? If so, please elaborate. _____
_____
_____

4. General Comments. What do you think should be changed to improve future reports? (Indicate changes to organization, technical content, format, etc.) _____
_____
_____

BRL Report Number _____ Division Symbol _____

Check here if desire to be removed from distribution list. ____

Check here for address change. ____

Current address: Organization _____
Address _____
_____

----------------------------------FOLD AND TAPE CLOSED----------------------------------

Director
U.S. Army Ballistic Research Laboratory
ATTN: SLCBR-DD-T(NEI)
Aberdeen Proving Ground, MD 21005-5066

OFFICIAL BUSINESS
PENALTY FOR PRIVATE USE $300
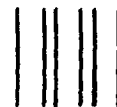
| NO POSTAGE |
| NECESSARY |
| IF MAILED |
| IN THE |
| UNITED STATES |

BUSINESS REPLY LABEL
FIRST CLASS   PERMIT NO. 12062 WASHINGTON D C

POSTAGE WILL BE PAID BY DEPARTMENT OF THE ARMY

Director
U.S. Army Ballistic Research Laboratory
ATTN: SLCBR-DD-T(NEI)
Aberdeen Proving Ground, MD 21005-9989

Director
U.S. Army Ballistic Research Laboratory
ATTN: SLCBR-DD-T(NEI)
Aberdeen Proving Ground, MD 21005-5066

- PASTE LABEL HERE -